WFPS-TME-78-103
OCTOBER, 1978
UC-20D

THERMAL AND HYDRAULIC ANALYSIS OF A CYLINDRICAL BLANKET MODULE DESIGN FOR A TOKAMAK REACTOR

A. Y. LEE

SPONSORED BY:

ORNL FUSION ENERGY DIVISION CONTRACT W-7405-ENG-26
SUBCONTRACT 7477

fusion power
systems department

Westinghouse Electric Corporation
P.O. Box 10864, Pgh. Pa. 15236

DISCLAIMER

WFPS-TME-78-103
UC-20D

THERMAL AND HYDRAULIC ANALYSIS OF A CYLINDRICAL BLANKET MODULE DESIGN FOR A TOKAMAK REACTOR

OCTOBER 1978

Prepared by: A. Y. Lee
A. Y. LEE
SYSTEM ENGINEERING

Approved by:
F. M. HECK
MANAGER
SYSTEM ENGINEERING

Approved by:
T. C. VARLOEN
MANAGER
ENGINEERING

Approved by:
C. A. FLANAGAN
MANAGER
MAGNETIC FUSION PROJECTS

fusion power systems department

Westinghouse Electric Corporation
P.O. Box 10864, Pgh. Pa. 15236

ACKNOWLEDGMENT

This work was performed for the Oak Ridge National Laboratory Fusion Energy Division, under U. S. Department of Energy Contract W-7405-ENG-26, Subcontract 7477. Reproduction, translation, publication, use, and disposal, in whole or in part, by or for the United States Government is permitted.

LEGAL NOTICE

Printed in the United States of America
Available from
National Technical Information Services
U.S. Department of Commerce
5285 Port Royal Road
Springfield, VA 22161
Price: Printed Copy $4.00; Microfiche $3.00

TABLE OF CONTENTS

LIST OF FIGURES

LIST OF TABLES

ABSTRACT

Various existing blanket design concepts for a tokamak fusion reactor were evaluated and assessed. These included the demonstration power reactors of ORNL, GA and others. As a result of this study, a cylindrical, modularized blanket design concept was developed. The module is a double-walled, stainless steel 316 cylinder containing liquid lithium for tritium breeding and is cooled by pressurized helium. Steady state and transient thermal conditions under normal and some off-design conditions were analyzed and presented. At the steady state reference operating point the maximum structure temperature is 452° C at the maximum stressed location and is 495° C at the less stressed location. The coolant inlet pressure is 54.4 atm, the inlet temperature is 200° C and the exit temperature is 435° C. The coolant could be utilized with a helium/steam turbine power conversion system with a cycle thermal efficiency of 30.8%.

1.0 INTRODUCTION

In the past several years conceptual designs of the blanket for a tokamak fusion reactor have been carried out by various organizations, such as that for the UWMAK of the University of Wisconsin, the demonstration power reactors of the Argonne and Oak Ridge National Laboratories, Doublets of GA and many others abroad. Lithium, helium, molten salts, etc., have been considered as the coolant; stainless steel, Inconel, etc., as the structural material. Early this year under the sponsorship of Oak Ridge National Laboratory, Westinghouse undertook a design study to evaluate and assess the various proposed concepts. Under the given guidelines of utilizing stainless steel as the structural material, helium as the coolant and stagnant (or slow moving) lithium as the breeding material, a new concept was proposed. The proposed concept consists of a narrow and long double-walled cylindrical module with a hemispherical front end. The outer cylinder wall serves as the front wall of the blanket region. The inner cylinder of the module contains liquid lithium for tritium breeding. The structure is cooled by pressurized helium gas which circulates through the annulus between the concentric cylinders.

Mechanical design, thermal-hydraulic and structural analyses were performed in support of this concept. The design was also assessed for performance, lifetime, maintenance, etc., under various operating conditions. A summary report on the results of the study is presented in Reference (1), the structural evaluations are described in Reference (2), and the design described in additional detail in Reference (3). The thermal-hydraulic analyses performed in support of the design study are presented in this report.

The thermal hydraulic design guidelines and requirements, model and method of analysis and the resulting blanket concept performance are given in the following sections of this report.

2.0 THERMAL-HYDRAULIC DESIGN GUIDELINES AND REQUIREMENTS

The scope of the present study was limited to consideration of a blanket design concept with the given set of design parameters discussed below. It was not intended to perform a comprehensive investigation but to develop a design concept for a tokamak reactor supported by adequate analysis consistent with the maturity of the design. The key design guidelines provided initially consisted of consideration of concepts incorporating stainless steel structure, liquid lithium moderator and gaseous helium coolant. The neutron wall loading was 2 - 4 MW/m^2 and the first wall particle heat flux is 0.5 - 1.0 MW/m^2. The design requirements pertaining to thermal design are as follows: the structural temperature limits are $\sim$ 400° C at the most highly stressed parts: $\sim$ 500° C at the lesser stressed parts and $\sim$ 550° C as the maximum. The helium exit gas temperature is to be as high as practical with the pumping power requirement of $\sim$ 2% of the blanket thermal power.

During the development of the design concept, some of the requirements given above were modified to be compatible with a power cycle to be used with the blanket coolant. This stems from the need to have a blanket coolant inlet temperature of at least $\sim$ 200° C and exit temperature greater than 400° C to operate a conventional helium/steam cycle with an acceptable cycle thermal efficiency. Since the blanket coolant exit temperature depends strongly on the first wall operating temperature, the first wall temperature limit was increased to 450° C from 400° C to increase the exit gas temperature. This new limit was found to be acceptable by a structural lifetime analysis (Reference 2). With the first wall structural temperature limit increased, the coolant flow required to cool the first wall to the temperature limit is greater with an inlet temperature of 200° C. The pumping power requirement was therefore increased from $\sim$ 2.0% to 2 - 2.5%. In the thermal design and analysis the maximum neutron wall loading of 4 MW/m^2 was considered. The corresponding particle heat flux on the first wall is 1 MW/m^2. The thermal design guidelines and requirements used in support of the concept development and subsequent assessment are summarized in Table 2.0-1.

TABLE 2.0-1

THERMAL DESIGN GUIDELINES AND PERFORMANCE REQUIREMENTS

Breeding Medium	Lithium
Structural Material	Austenitic stainless steel (SS 316)
Coolant	Pressurized helium
Structural Temperature Limits	$\sim$ 450° C High stressed structure
	$\sim$ 500° C Low stressed structure
	$\sim$ 550° C maximum
Neutron Wall Loading	4 MW/m^2
First Wall Particle Heat Flux	1 MW/m^2
Coolant Temperatures	Inlet @ 200° C
	Outlet as high as practical
Pumping Power	2 - 2.5% of blanket thermal power (at 70% efficiency)
Pulse Cycle	20 minutes with 95% duty

3.0 BLANKET MODULE DESIGN DESCRIPTION

The blanket design consists of cylindrical modules with a hemispherical front end which serves as the first wall of the blanket region. The outer diameter of the outer cylinder of a module is $\sim$ 10 cm (4") and the overall length of the module is 75 cm (29.5"). A schematic of the module concept is shown in Figure 3.0-1. The coolant enters the outer flow channel at the base of the module, turns around at the center of the front wall and exits from the inner flow channel also at the base of the module. The inner cylinder contains the liquid lithium which is considered stagnant during reactor operation for purpose of the analysis. The outer 15 cm of the inner cylinder contains a stainless steel shield which also aids the tritium breeding in the module.

The wall thickness of each of the cylinders is 1.57 mm (.062"). The counter-flow coolant streams are separated by a flow baffle which is also a double-walled cylinder with a stagnant helium insulating gap between the outer and the inner baffles. The wall thickness of the baffles is about 0.38 mm (0.015"). The stagnant helium gap required was determined to be about 2.28 mm (.090") which is needed to isolate the two flow paths so that the heat from the inner path would not be transferred to the outer path and heat up the coolant before it reaches the turn-around point.

The sizes of the flow gaps were determined to provide simultaneously a first wall temperature below the limit of 450° C and a pumping power of below the limit of 2.5% of the blanket thermal power. For this design, the outer gap at the straight section of the cylinder is 1.27 mm (.050"). At the spherical section the gap is tapered to 0.76 mm (.030") at the turn-around to further increase the coolant velocity. The inner gap is however, 0.25 cm (.100") uniformly throughout the flow path.

The modules are arranged in six different orientations to form a D-shape sector surrounding the plasma as shown in Figure 3.0-2. An enlarged view of

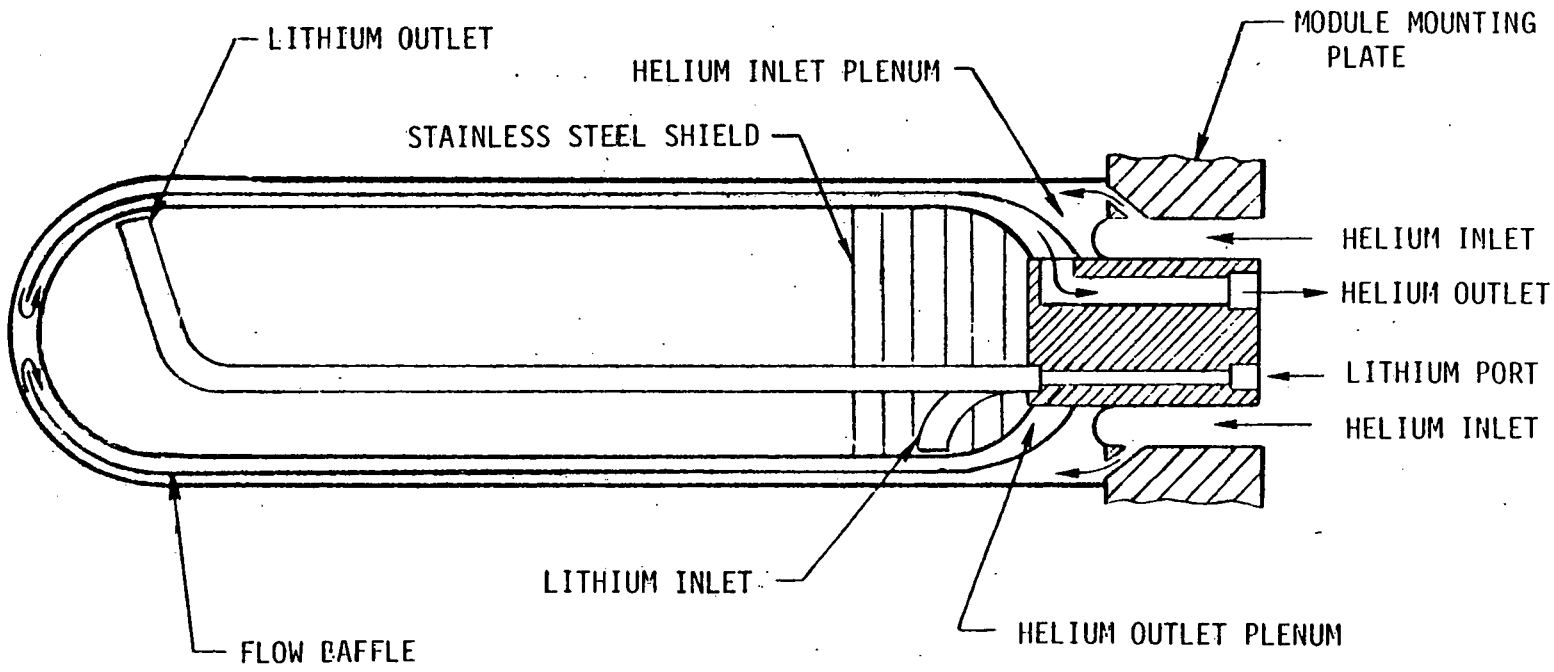

Figure 3.0-1. Schematic of Cylindrical Module Concept

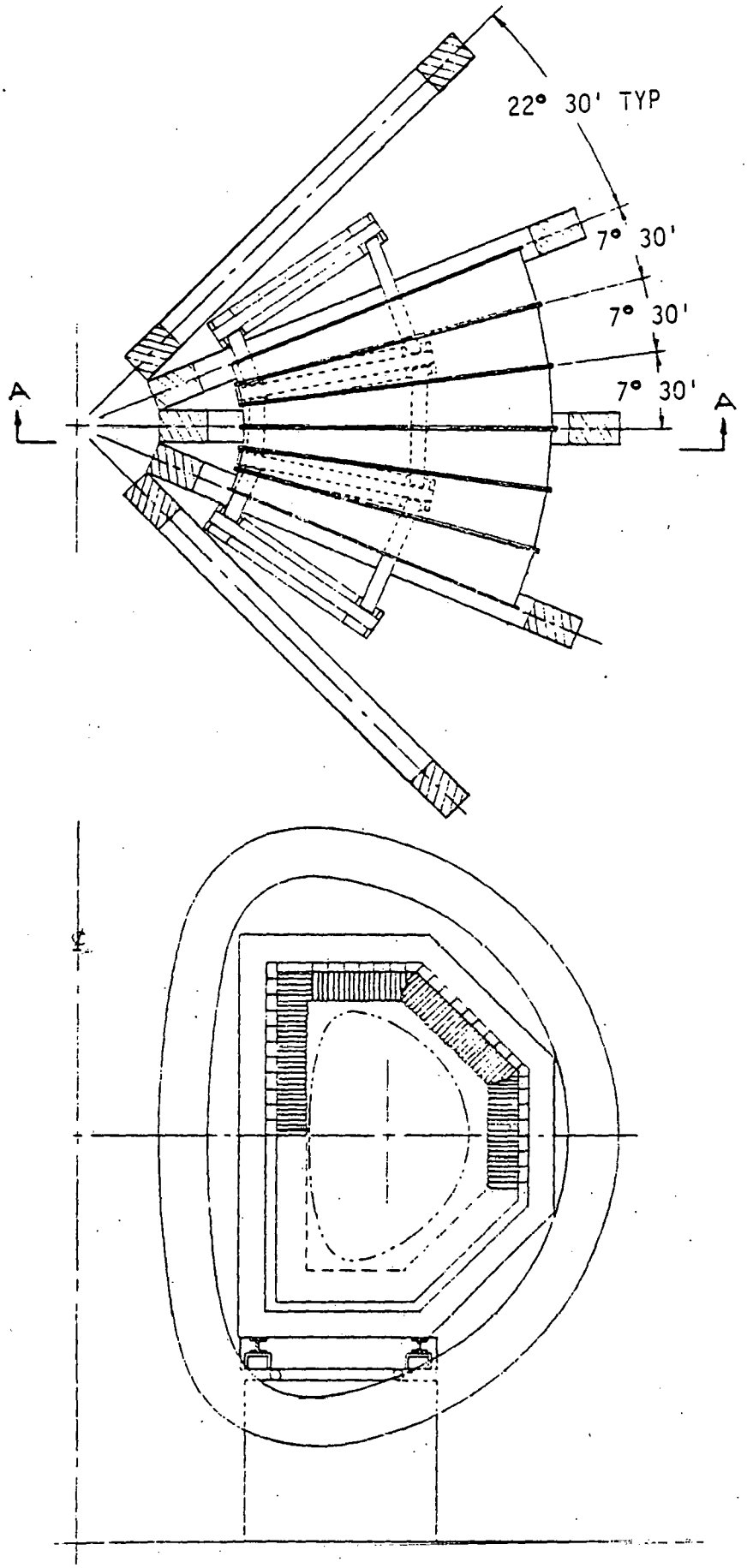

Figure 3.0-2. Plan and Side Views of Blanket Module Assembly

the six sectors shown in Figure 3.0-2 is shown in Figure 3.0-3. The interstitial spaces between the modules may be fitted with inserts to minimize direct streaming of high energy neutrons against the shield and the support structures. The major dimensions and the module support structures are shown in Figure 3.0-4. This figure also shows the common manifolds for the helium and the lithium. The details of the mechanical design, structural analysis summary, assembly and disassembly methods are given in Reference (1).

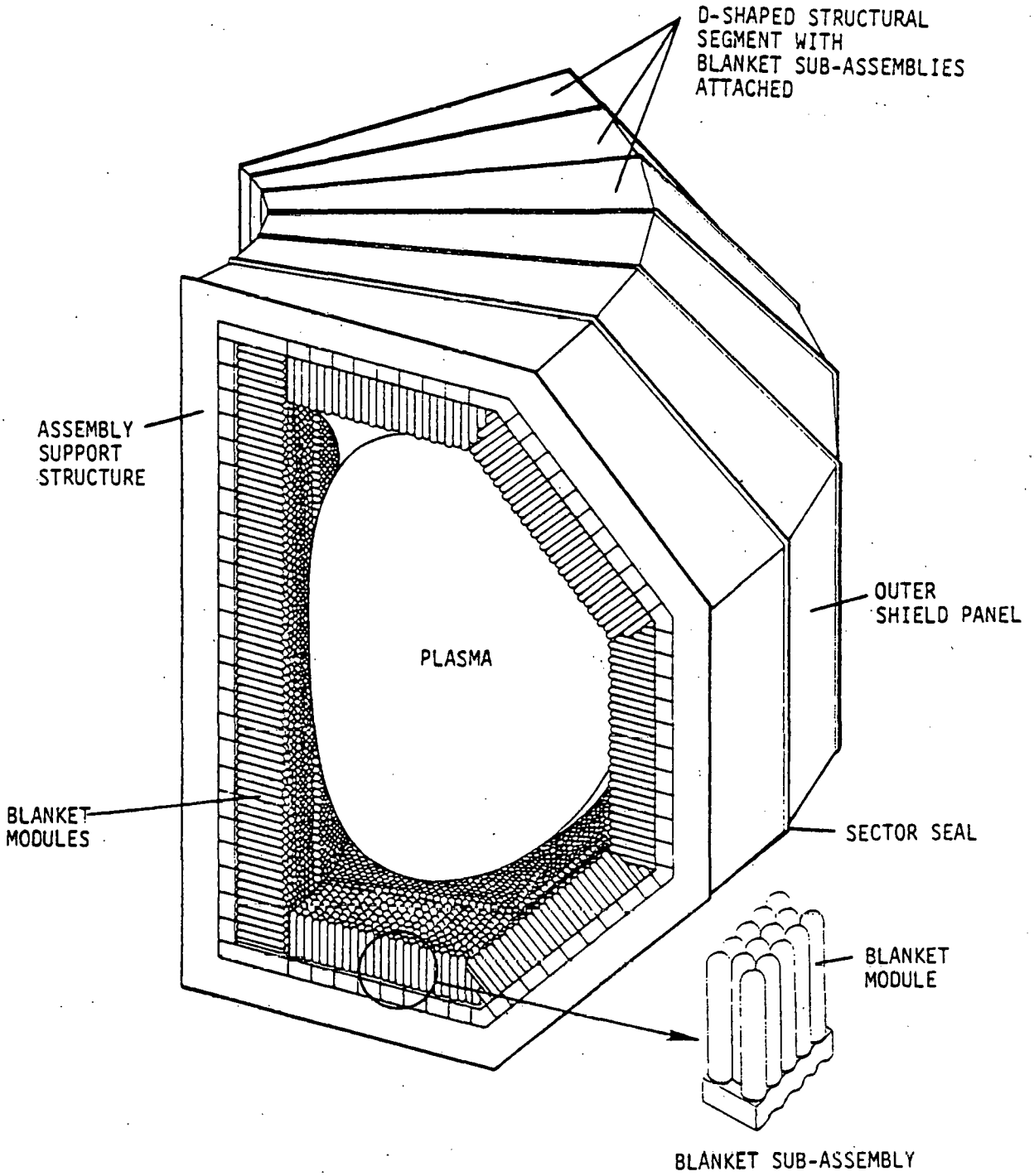

Figure 3.0-3. Enlarged View of Blanket Sectors Assembly

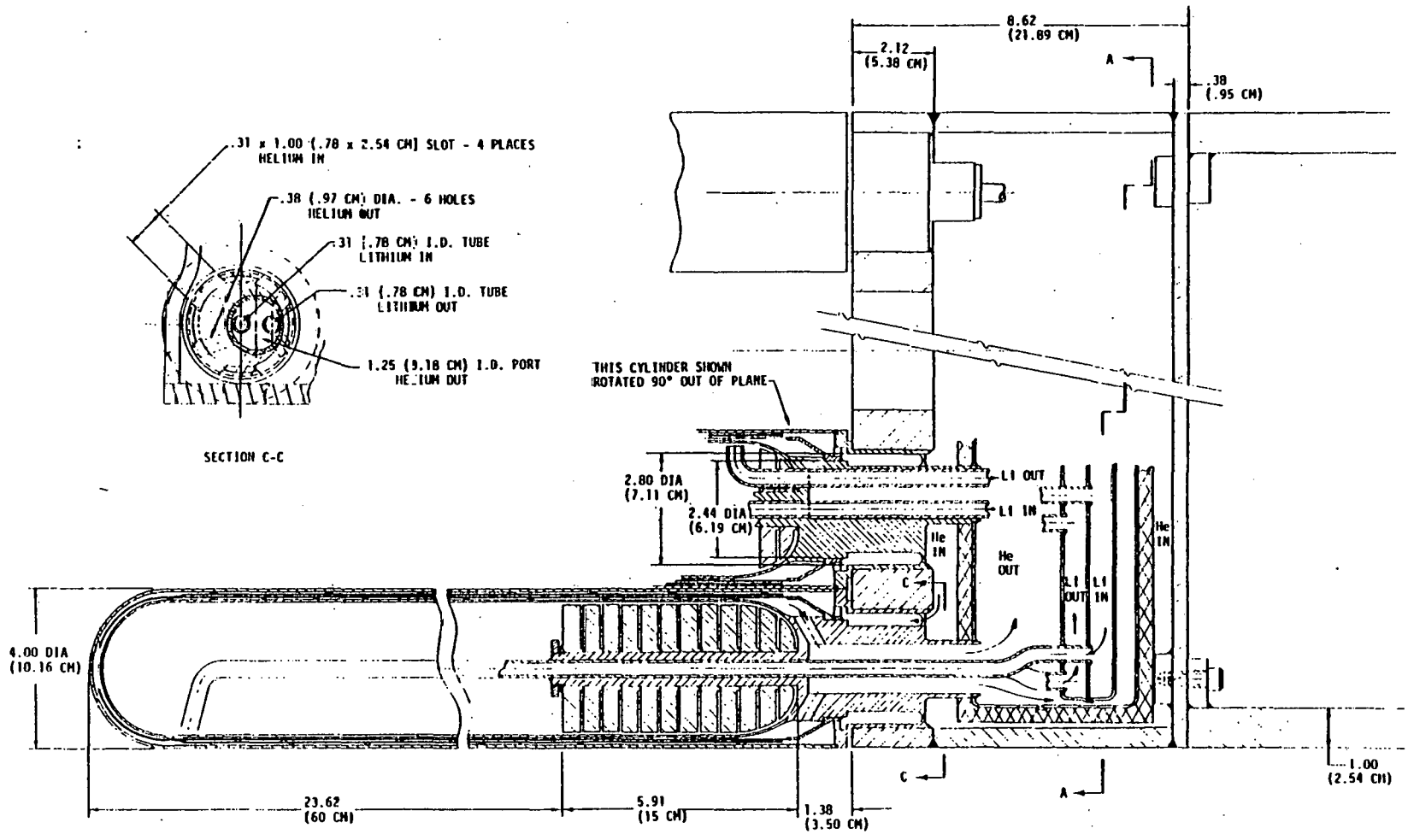

Figure 3.0-4. Support Assembly of Cylindrical Module Concept

4.0 MODEL AND METHOD OF ANALYSIS

The thermal and hydraulic performance of the module was analyzed by solving the heat conduction equation for the solid materials and the one-dimensional conservation equations for the helium coolant flow. The heat conduction equation and the boundary conditions are:

$$\frac{\partial}{\partial x}\left(k\frac{\partial T}{\partial x}\right) + \frac{\partial}{\partial y}\left(k\frac{\partial T}{\partial y}\right) + \frac{\partial}{\partial z}\left(k\frac{\partial T}{\partial z}\right) = \rho c_p \frac{\partial T}{\partial \theta} + Q''' \qquad (1)$$

$$-k\frac{\partial T}{\partial n} = h\,(T - T_{He}) \qquad \text{@ coolant channel wall} \qquad (2)$$

$$-k\frac{\partial T}{\partial n} = Q \qquad \text{@ outer wall with specified heat flux} \qquad (3)$$

The fluid flow conservation equations are:

$$\text{Continuity} \qquad \frac{\partial G}{\partial x} + \frac{\partial \rho}{\partial \theta} = 0 \qquad (4)$$

$$\text{Energy} \qquad \frac{\partial (GH)}{\partial x} + \frac{\partial (\rho H)}{\partial \theta} - \frac{1}{J}\frac{\partial p}{\partial \theta} - \frac{QP}{A} = 0 \qquad (5)$$

$$\text{Momentum} \qquad \frac{\partial p}{\partial x} + \frac{1}{g}\frac{\partial G}{\partial \theta} + \frac{1}{g}\frac{\partial (G^2 v)}{\partial x} + \tau = 0 \qquad (6)$$

Where τ is a frictional term defined by $\frac{2f|G|Gv}{gD}$ which acts opposite to the direction of flow. In Equation (2) and (3) the n is the outward normal to the solid surface boundary. The right hand side of Equation (2) is the heat flow to the coolant and is the term Q shown in Equation (5). This term is the coupling quantity between the heat conduction and the fluid flow analyses.

The definitions of the symbols in the equations are given in the notations section of this report (Section 7.0). In addition to the above questions, the equation of state for the coolant fluid is needed to determine the fluid properties. The thermal and transport properties for the helium fluid are supplied by a set of computer subroutines[4] for the computations.

Equation (1) is formulated for a multi-dimensional heat conduction body. Since the blanket module is axially symmetric, radial and axial heat flow are therefore considered in the analysis. The fluid flow equations are formulated for a one-dimensional flow along the flow channel in the model. The counter-flow characteristic of the coolant flow in the module is accurately modeled.

The above equations are solved by an implicit finite difference procedure on a larger scale computer. Temperature dependent material and coolant properties are considered in the calculations.

The heat transfer coefficients in the cooling channels are computed by the well known Dittus-Boelter[5] correlation for turbulent flow as shown below:

$$Nu = .023\ (Re)_f^{.8}\ (Pr)_f^{.4} \tag{7}$$

The fluid properties are evaluated at the bulk conditions. The friction factor for pressure drop calculations is evaluated by the Koo[6] correlation for turbulent flow as shown below:

$$f = 0.0014 + \frac{0.125}{Re^{0.32}} \tag{8}$$

The above correlations are, however, developed for straight and smooth tubes. Since the flow baffles in this module design have individual stand-offs for spacing, these "spoilers" would enhance heat transfer but increase frictional loss. A multiplier greater than unity was therefore used to increase the heat transfer coefficient and friction factor obtained from the above correlations. Numerous experiments have been performed to measure heat transfer and

friction data with artificial roughness inside a tube or annulus. Reference (7) contains a detailed survey of work done. The augmentation ranges from tens of percent to several hundreds percentage over the smooth surface data. Unfortunately, none of these data were obtained with a flow path similar to the one being considered. In this conceptual design analysis, a conservative multiplier of 1.40, applied to both heat transfer and friction loss, was used.

The analysis model for the module is shown in Figure 4.0-1. Considering the condition of axial symmetry, the model consists of a 5° sector of the cylinder. The nodal pattern on the R - Z coordinate plane is shown in the figure. The straight section of the cylinder is divided into ten axial increments and the spherical portion is divided into four circumferential increments (the first wall has five increments). The lithium region is further divided into three radial increments. Radial and axial heat conductions in the solid materials are included in the model. The helium enters the outer gap channel at the base of the cylinder, turns around at the tip of the hemisphere into the inner gap channel and also exits at the base of the cylinder. This is a counter flow system with potential heat transfer from the inner gap to the outer gap. In order to minimize such thermal "short-circuiting" a stagnant helium gap is provided between the two baffles. Calculations indicated that a stagnant helium layer in the order of 0.22 cm (0.090") would act like an essentially ideal insulation. A gap of this dimension was included in the model for analysis (this gap was not shown in the design layouts).

The heat transfer coefficient and pressure loss at the turn-around are areas of uncertainty in the analysis, since there are not any applicable empirical data or correlations for this particular type of flow geometry. It is expected that a high degree of turbulence will exist at the center of the dome and cross-flow may occur at the turn-around. The heat transfer coefficient at the center of the dome may even be higher than that at the exit of the outer flow channel due to the jet mixing action. It was therefore, assumed that the heat transfer coefficient there would be about 50% higher than that at the outer flow channel exit. For the pressure loss at the turn-around it was calculated that one velocity head is lost around the first 90° turn at the exit of the outer flow path and 0.8 velocity head is lost at the second 90° turn into the inner flow channel. The calculations considered the turns and the area changes in the flow channel.

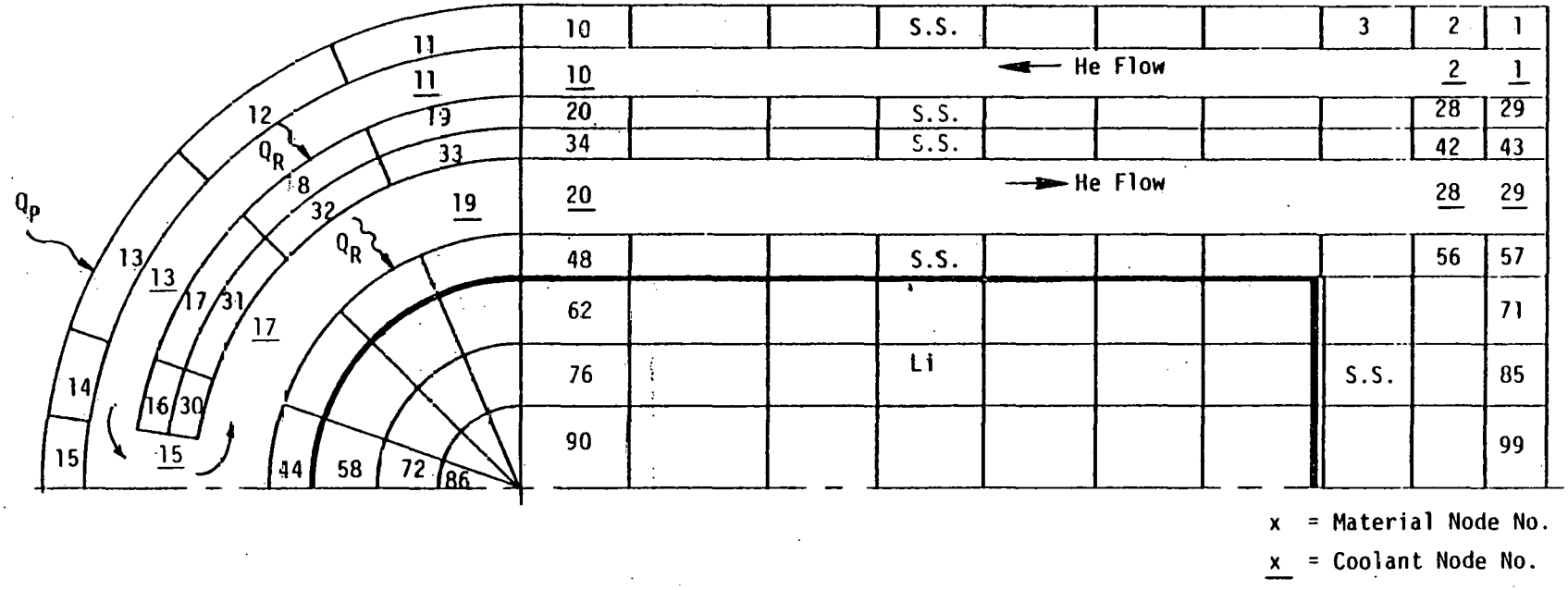

Figure 4.0-1. Thermal and Hydraulic Finite Difference Analysis Model of Module

These values were used in the model for the thermal and hydraulic performance analysis of this module design.

The incident heat flux of 1 MW/m^2 on the outer surface of the hemisphere was assumed to vary according to a cosine function distribution. The cosine angle is that between the radius of the sphere and the axis through the center line of the cylinder. The integration of this heat input distribution over the curved surface equals that through the base of the hemisphere. The internal heat generation rates of the stainless steel and the lithium due to a neutron wall loading of 4 MW/m^2 used in the analyses were obtained from a preliminary nuclear calculation and are shown in Figure 4.0-2. The neutronic performance of the blanket was evaluated using the discrete-ordinate transport theory code ANISN, and the heating and T breeding rates were computed with the AAP code. The ANISN calculations were done with a coupled 26 neutron and 16 group photon cross section library applied in the P_3S_6 approximation. The geometric model was based on a horizontal cut through the torus in the equatorial plane, and one-dimensional radial representation, with the center of coordinates placed at the center of the machine. Zero transverse leakage was specified.

As shown in Figure 4.0-1 the model consists of a total of 99 internal material nodes (only a few node numbers at the key locations are shown in the figure) and 29 helium flow nodes (the node numbers are underlined). The diameter of the hole at the turn-around was taken to be 2.5 cm (1"). Thermal radiation (Q_R) between the structure surfaces are included in the model.

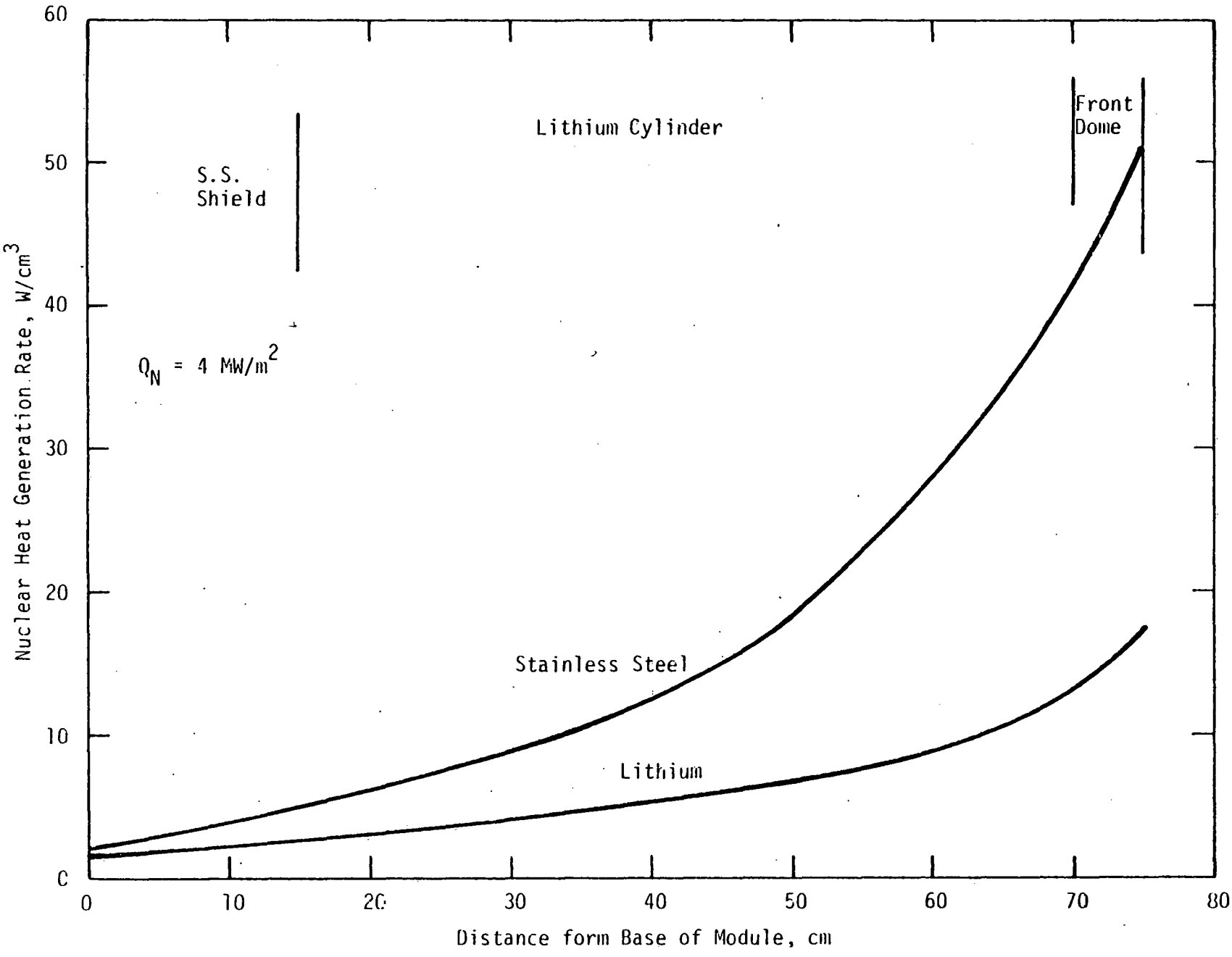

Figure 4.3-2. Nuclear Heat Generation Rates of Materials in Module

5.0 THERMAL-HYDRAULIC PERFORMANCE OF THE BLANKET MODULE

With the design guidelines, requirements and model of analysis described previously, the thermal and hydraulic performance of the blanket module was analyzed. The module operating limits were first determined. From these limits a reference operating condition was selected. The analysis results provide thermal inputs to the structural evaluations of the module.

Preliminary mechanical design was carried out to determine the overall size of the module. A $\sim$ 10 cm (4") outer diameter module was selected for initial evaluation. The analysis considered the following assumptions besides those discussed in the model development (Section 4.0):

(1) Since the duty cycle is 95% with a burn-time of 19 minutes, the thermal conditions of the module would reach a steady state condition shortly after the initiation of the plasma. Steady state calculations were performed to determine the thermal conditions of the module. Transient calculations were performed to determine the transient response of the module during plasma-off and the early part of the plasma-on period.

(2) The pumping power requirement of the module includes the frictional losses inside the flow channels and the losses at the baffle turn-around. The losses in the headering, the piping systems and the module entrance and exit losses are not included. A pumping efficiency of 70% was assumed in the pumping power calculation.

(3) Neutron wall loading is 4 MW/m^2 and the associated particle heat flux is 1 MW/m^2.

(4) The thermophysical properties of the materials are temperature dependent. The irradiation effects on the properties are not included in the analysis.

5.1 PERFORMANCE OF THE 10 cm DIAMETER MODULE

Initial parametric calculations were carried out to determine the sizes of the flow gaps to obtain the desired performance from the module. The outer flow gap was then selected to be 0.125 cm (.050") and the inner flow gap was selected to be .250 cm (.100"). The first model developed had a uniform outer gap of 0.125 cm along the full length of the channel including the nose region. Since the peak particle heat flux is maximum at the top of the dome, the calculated first wall circumferential temperature variation was appreciable, even with the converging flow channel area toward the center of the dome. The outer gap size at the nose region was therefore, reduced to increase the heat transfer coefficient in that area. This not only reduced the circumferential temperature variation, but also lowered the peak first wall temperature.

With various outer gap size distribution at the nose (the gap sizes at the cylindrical portion of the outer flow channel remains the same at .125 cm and the inner flow channel gap is uniform at .250 cm), the steady state thermal conditions of the module were calculated using different helium inlet temperatures, inlet pressures and flow rates. The results are summarized in Table 5.1-1.

The performance curves with helium inlet temperature of 100° C are plotted in Figure 5.1-1. In this figure the maximum first wall temperature was plotted against the pumping power requirement and the helium exit temperature was plotted against the maximum first wall temperature. The short dashed lines are the performance curves with a constant outer flow gap at the nose region and helium inlet pressure of 35 atm. Case 1 of Table 5.1-1 is shown by the circles on the curves. In order to operate with the maximum first wall temperature at 450° C, the pumping power requirement would be increased to $\sim$ 1.3% which is satisfactory, but the helium exit would be lowered to $\sim$ 350° C

TABLE 5.1-1

SUMMARY OF THERMAL PERFORMANCE OF MODULE

CASE	P_{IN} atm	T_{IN} ° C	W_{IN} g/s	T_{OUT} ° C	MAXIMUM FIRST WALL TEMP ° C	MAX. INNER CYLINDER TEMP ° C	LITHIUM TEMP MIN ° C	LITHIUM TEMP MAX ° C	PUMPING POWER @ 70% eff. %	OUTER GAP DISTRIBUTION AT NOSE
1	35.0	100	26.2	420	502	483	433	616	0.70	A**
2	35.0	100	26.2	420	445	480	431	613	1.50	B
3	54.4	100	26.2	420	443	480	431	613	0.71	B
4	35.0	100	26.2	420	415	483	433	616	1.75	C
5	54.4	100	26.2	420	415	483	433	616	0.90	C
6	35.0	200	35.0	435	452	492	462	627	5.27	C
7*	54.4	200	35.0	435	452	492	462	627	2.20	C
8	68.0	200	35.0	435	452	492	462	627	1.43	C
9	54.4	250	43.7	435	466	492	473	627	4.82	C
10	68.0	250	43.7	435	466	492	473	627	3.07	C
11	54.4	300	57.3	437	485	493	486	629	12.31	C
12	68.0	300	57.3	437	485	493	486	629	7.71	C

* Reference design

** Gap distribution is given at end of the fluid nodes 11, 12, 13 and 14 (see model in Figure 4.0-1):

A = Constant @ .127 cm

B = .127 - .102 - .076 - .152 cm

C = .102 - .076 - .076 - .076 cm

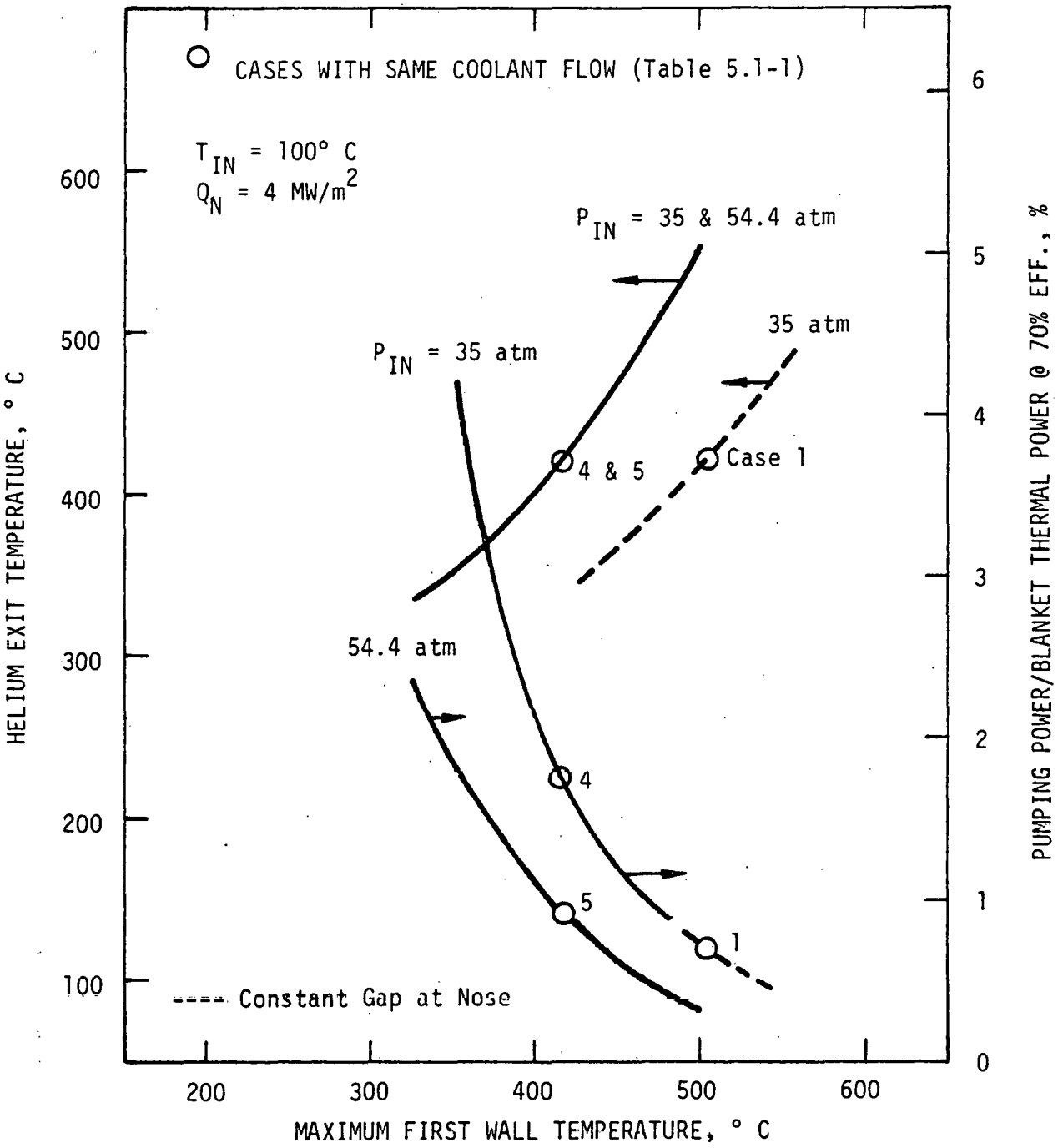

Figure 5.1-1. Steady State Performance Curves of Module with T_{IN} = 100° C

which is considered too low for reasonable power conversion efficiency. Reducing the outer gap distribution at the nose region to the values as shown for cases 4 and 5 (Table 5.1-1) the performance curves are shifted to the left in the figure (the solid lines). The cases 4 and 5 are shown by the circles on the new performance curves. From these new performance curves it is seen that if the module is operated with the maximum first wall temperature at $\sim$ 450° C, the helium exit temperature would be $\sim$ 470° C and the pumping power requirement would be $\sim$ 1.3%, if the helium inlet pressure is 35 atm and less than 1.0%, if the helium inlet pressure is 54.4 atm.

The curves on this figure clearly illustrate the sensitivity to the outer gap distribution at the nose region and the helium inlet pressure on the performance of this module design. The outer gap distribution at the nose region shown for the cases 4 and 5 was therefore, selected for the reference design and was used in the subsequent performance analyses.

Thermal conditions with higher helium inlet pressures and higher inlet temperatures were also calculated to study the effects of these parameters. The results are shown as cases 6 to 12 in Table 5.1-1. As expected, increasing the helium inlet temperature requires higher flow rate to cool the structures to within the specified temperature limits. Consequently, the required pumping power is higher, unless the helium pressure is raised to increase the gas density. Results of structural analysis indicated that a helium pressure of 54.4 atm (800 psia) is still acceptable for this module design. This pressure was therefore, selected as the reference helium inlet pressure.

For power conversion cycle performance consideration the helium inlet temperature of 100° C is considered too low. With the blanket exit temperature limited to about 440° C (by the maximum structural temperature limits), an inlet temperature of at least 200° C is about the level to have a reasonable helium/steam power conversion cycle. With the coolant exit temperature at the 450° C level, a direct helium gas turbine cycle for power conversion would result in an unreasonabley low cycle thermal efficiency. The helium inlet temperature of 200° C was therefore selected to be one of the reference operating conditions.

It should be noted that comprehensive optimization has not been carried out to obtain the most optimum operating conditions. The above can be considered as the nominal values for a base case.

5.2 REFERENCE DESIGN OPERATING CONDITIONS

As discussed in the previous section the reference helium inlet pressure and temperature are 54.4 atm and 200° C, respectively. The steady state operating characteristics of this module design at different coolant flow rates are shown in Figure 5.2-1. In this figure the maximum inner cylinder temperature and the corresponding first wall temperature at the same coolant flow were plotted against the pumping power requirement (instead of the flow rates). The helium exit temperature was plotted against the maximum first wall temperature. The allowable operating region is therefore, to the left of 500° C maximum inner cylinder temperature or to the left of 450° C maximum first wall temperature. The pumping power requirement increase is very rapid as the maximum structure temperature is lowered. The maximum operating point is indicated by the circles on the curves. This represents case 7 of Table 5.1-1 which was selected as the reference case. The maximum first wall temperature is 452° C, the maximum inner cylinder is 492° C, the helium exit temperature is 435° C and the required pumping power is 2.2%.

The steady state nodal temperature distribution of the module is shown in Figure 5.2-2. In this figure, only the temperatures at the key locations are shown, although temperatures at all nodal points were computed. The maximum first wall temperature occurs at a point about 30° from the module central axis. This is the result of a combination of the increasing flow velocity (hence heat transfer coefficient) going toward the turn-around point and the decreasing outer surface heat flux away from the top of the hemisphere. The minimum and maximum lithium temperatures are 461° C and 627° C, respectively. The lithium is therefore, maintained in the molten state. The maximum stainless shield temperature is 559° C. Since the shield is not a structural member, this temperature level is considered satisfactory.

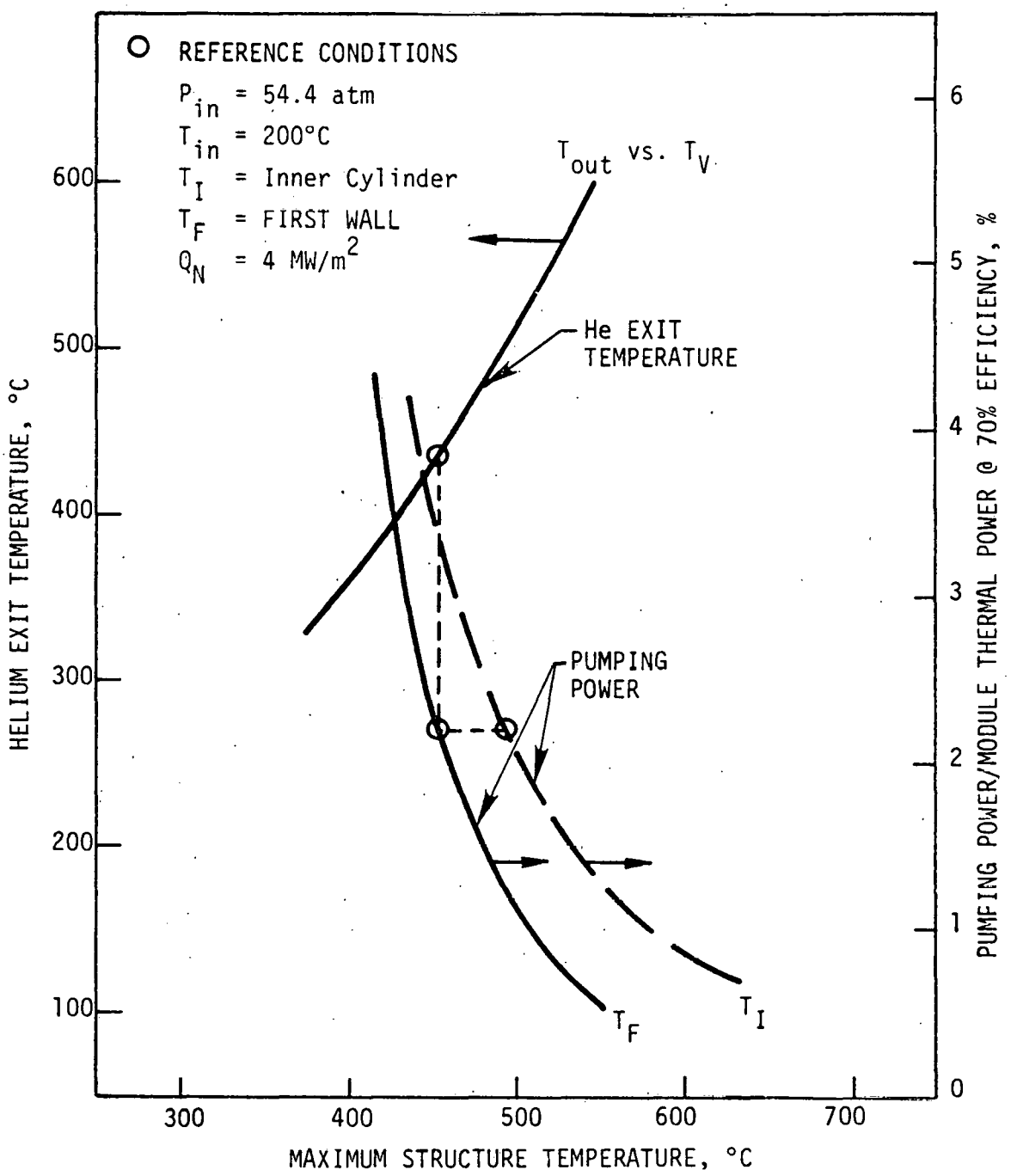

Figure 5.2-1. Steady State Performance Curves of Module with T_{in} = 200°C.

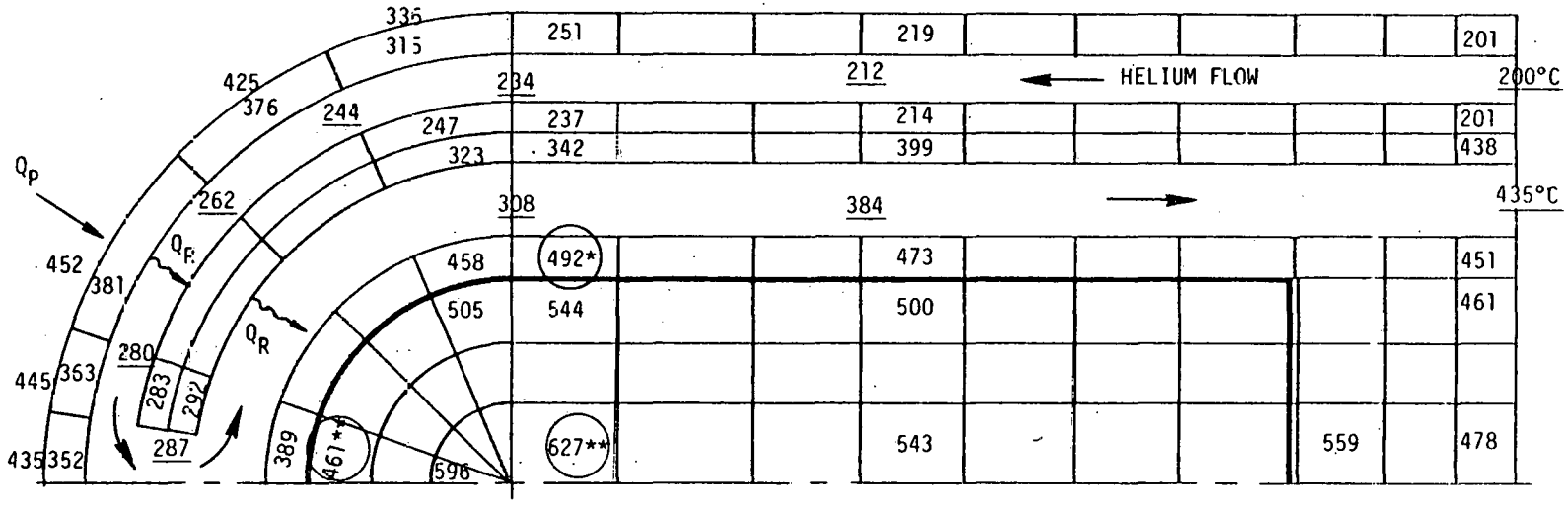

Helium Inlet Pressure = 54.4 Atm (800 psia)
Helium Inlet Temperature = 200°C
Neutron Wall Loading = 4 MW/m^2

*Max. S.S. Structure Temp.
**Min. & Max. Li Temp.

xx = Material Temp, °C
xx = Coolant Temp, °C

Figure 5.2-2. Steady State Material and Coolant Temperatures of Blanket Module at Reference Operating Conditions

The helium coolant axial temperature and the cylinder wall average temperature distributions are shown in Figure 5.2-3. The first wall temperature on the hemisphere is also shown in the figure. The coolant temperature rise in the outer cooling channel is 85° C or 36% of the total coolant temperature rise. If the flow baffles were not well insulated, the coolant in the outer gap flow channel would be heated to a higher temperature when it reaches the hemisphere. More coolant flow, therefore, would be required to cool the first wall to the temperature limit or the helium inlet temperature would need to be lowered. This would compromise the module thermal performance. It is therefore, important to have adequate insulation between the two counter-flowing streams.

The reference thermal parameters of the module are summarized as shown in Table 5.2-1.

5.3 POWER CONVERSION SYSTEM

With a blanket coolant outlet temperature of 435° C and an inlet temperature of 200° C, a conventional regenerative steam turbine cycle could be used for power conversion. The cycle diagram for the steam turbine with one extraction point is shown in Figure 5.3-1 (a). The temperature-enthalpy plot for the steam generator portion is shown in Figure 5.3-1 (b). The feed water inlet temperature (point a) was chosen at 93° C (200° F). The temperature difference at the pinch point b was taken to be 20° C and that at the steam generator exit (point d) was taken to be 15° C. With these temperature levels the maximum steam pressure was determined to be 23.8 atm (350 psia) and the extraction point pressure 0.68 atm (10 psia). The condenser pressure is assumed to be 3.38 kPa (1" Hg abs.). Assuming a turbine stage efficiency of 80% before the extraction point and 75% after the extraction point, the cycle thermal efficiency was calculated to be 30.8%. The heat supplied to the cycle per kw-hour of work delivered is 11.66 MJ.

Other power conversion cycles were also briefly investigated, such as the closed-loop helium gas turbine or dual pressures steam turbine cycles. These cycles offer much lower thermal efficiency due to the low coolant temperature and were not pursued further.

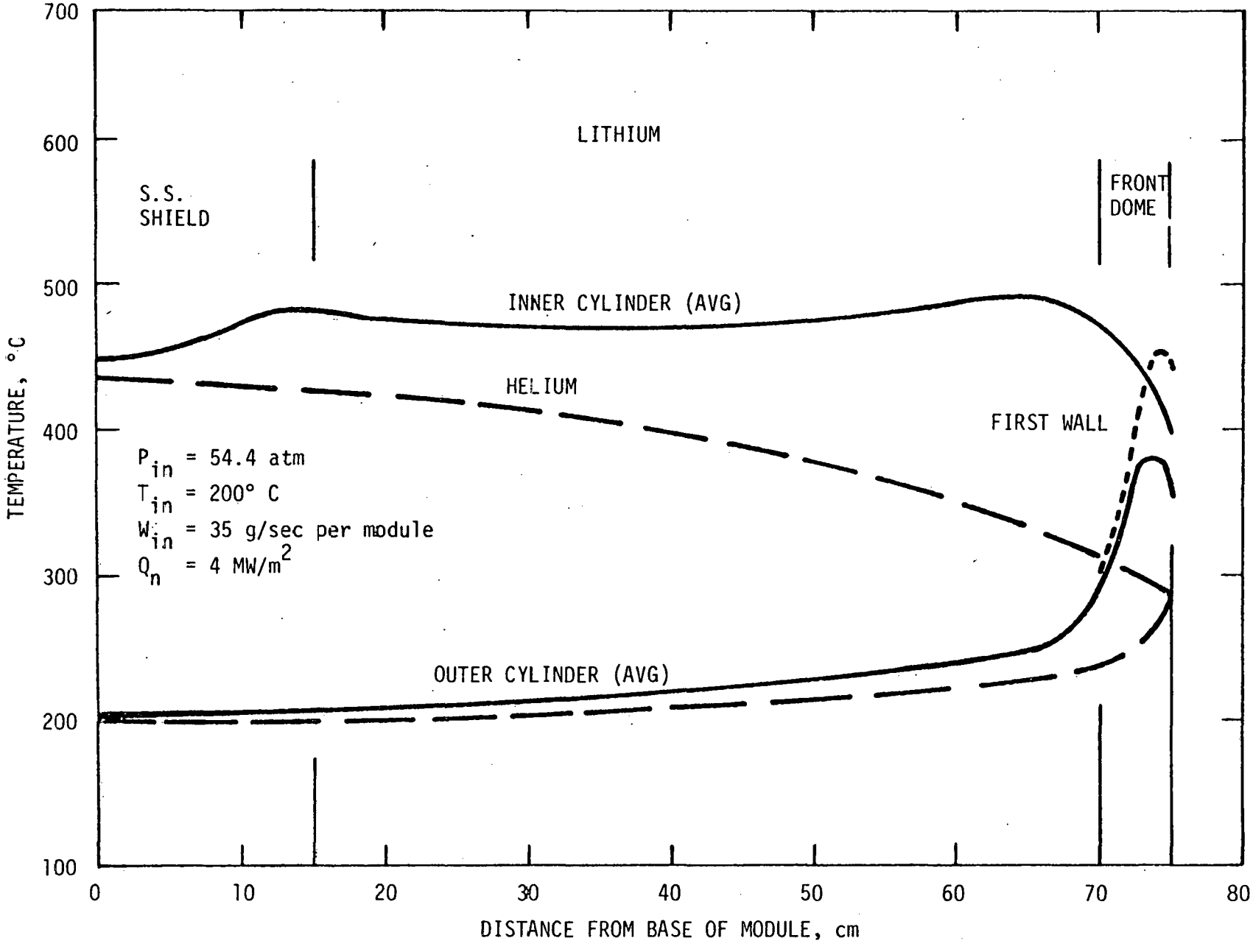

Figure 5.2-3. Axial Temperature Profiles of Helium and Structural Cylinders at Reference Operating Conditions

TABLE 5.2-1

REFERENCE THERMAL PERFORMANCE PARAMETERS OF THE BLANKET MODULE

Helium inlet pressure	54.4 atm
Helium inlet temperature	200° C
Helium outlet temperature	435° C
Helium temperature at turn-around	287° C
Maximum first wall temperature	452° C
Minimum outer cylinder temperature	201° C
Maximum inner cylinder temperature	492° C
Minimum inner cylinder temperature	389° C
Maximum lithium temperature	627° C
Minimum lithium temperature	461° C
Maximum stainless steel shield temperature	559° C
Minimum stainless steel shield temperature	461° C
Helium flow rate per module	35 g/sec
Maximum heat tranfer coefficient at nose region	1.59 W/cm^2-C
Pressure drop at outer gap channel	56.6 kPa
Pressure drop at turn-around	38.6 kPa
Pressure drop at inner gap channel	0.69 kPa
Module thermal power	45.1 kw
Module pumping power @ 70% efficiency	2.2 %

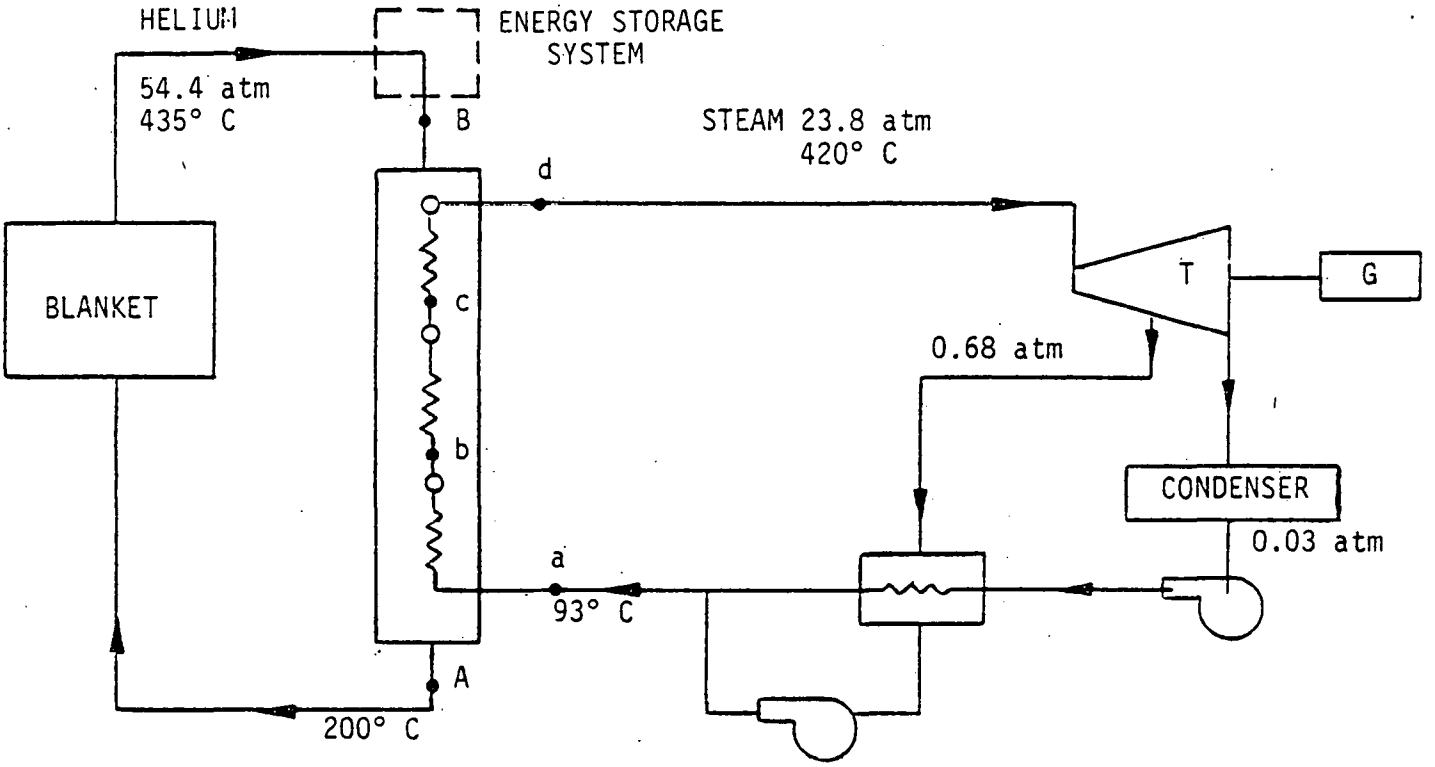

(a)

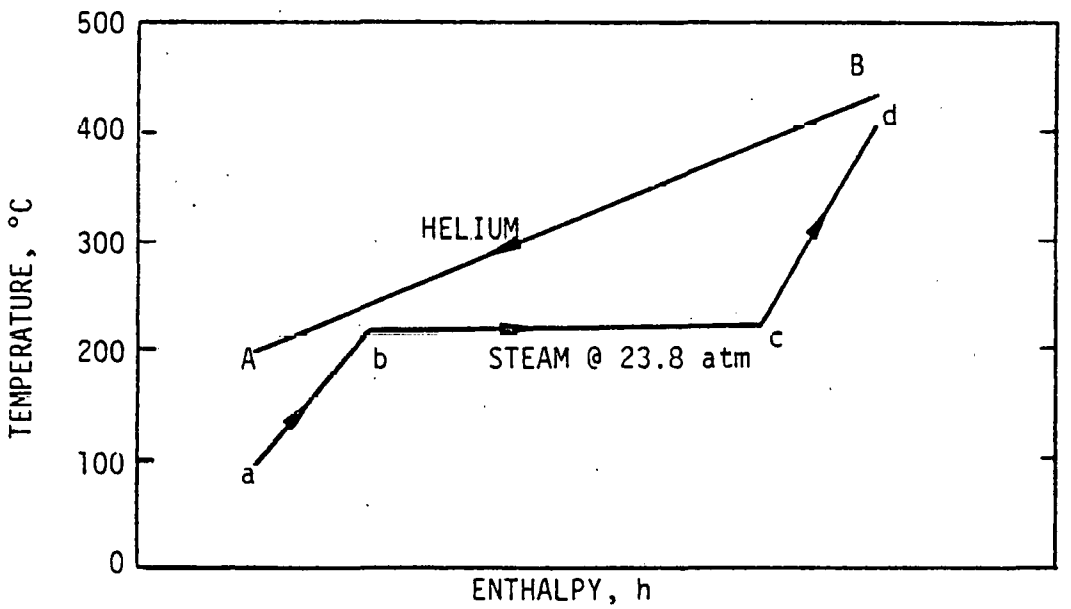

(b)

Figure 5.3-1. Helium/Steam Power Conversion Cycle Configuration.

Due to the pulsed operating characteristic of a tokamak, the coolant exit temperature would fluctuate during a cycle. A buffered energy storage system would be required, so that the steam cycle can be operated at a steady state condition. The details of the energy storage system and its effect on the power conversion system performance were considered to be outside the scope of this study and have not been analyzed.

5.4 PERFORMANCE DURING PLASMA-OFF AND PLASMA-ON TRANSIENTS

The reference duty cycle for this blanket design consists of a 19 minute plasma-on and a one minute plasma-off period (95% duty cycle). Assuming a step change in thermal loadings as the plasma is terminated and initiated, the transient temperatures of the structure, lithium and the helium during the plasma-off and the subsequent plasma-on periods are shown in Figure 5.4-1. As expected, the first wall responds rapidly to the particle heat flux due to the thin-walled structure. The lithium is cooled to about 220° C at the end of the one minute of plasma-off time and is still in the molten state. The helium exit temperature drops to about 300° C from 435° C. This coolant temperature fluctuation would affect the operation of the power conversion system as discussed in the previous section.

After the plasma burn is resumed, it is seen from the figure that it takes about 2 to 3 minutes for the helium and the material temperatures to reach the previous steady state values. As long as the plasma-on time is longer than three minutes, changing the burn time of a cycle will have no effect on the steady state thermal conditions of the module. On the other hand, if the plasma-off period is longer than one minute, the helium exit temperature would continue to drop, degrading the efficiency of the power conversion system. If the coolant inlet temperature could be maintained above 180° C (the melting point of lithium) with a longer plasma-off time, the lithium at the cold spot may not reach the solidification point. It should be noted that the decay heat during the plasma-off period was not included in the calculations. The results obtained, therefore, are conservative.

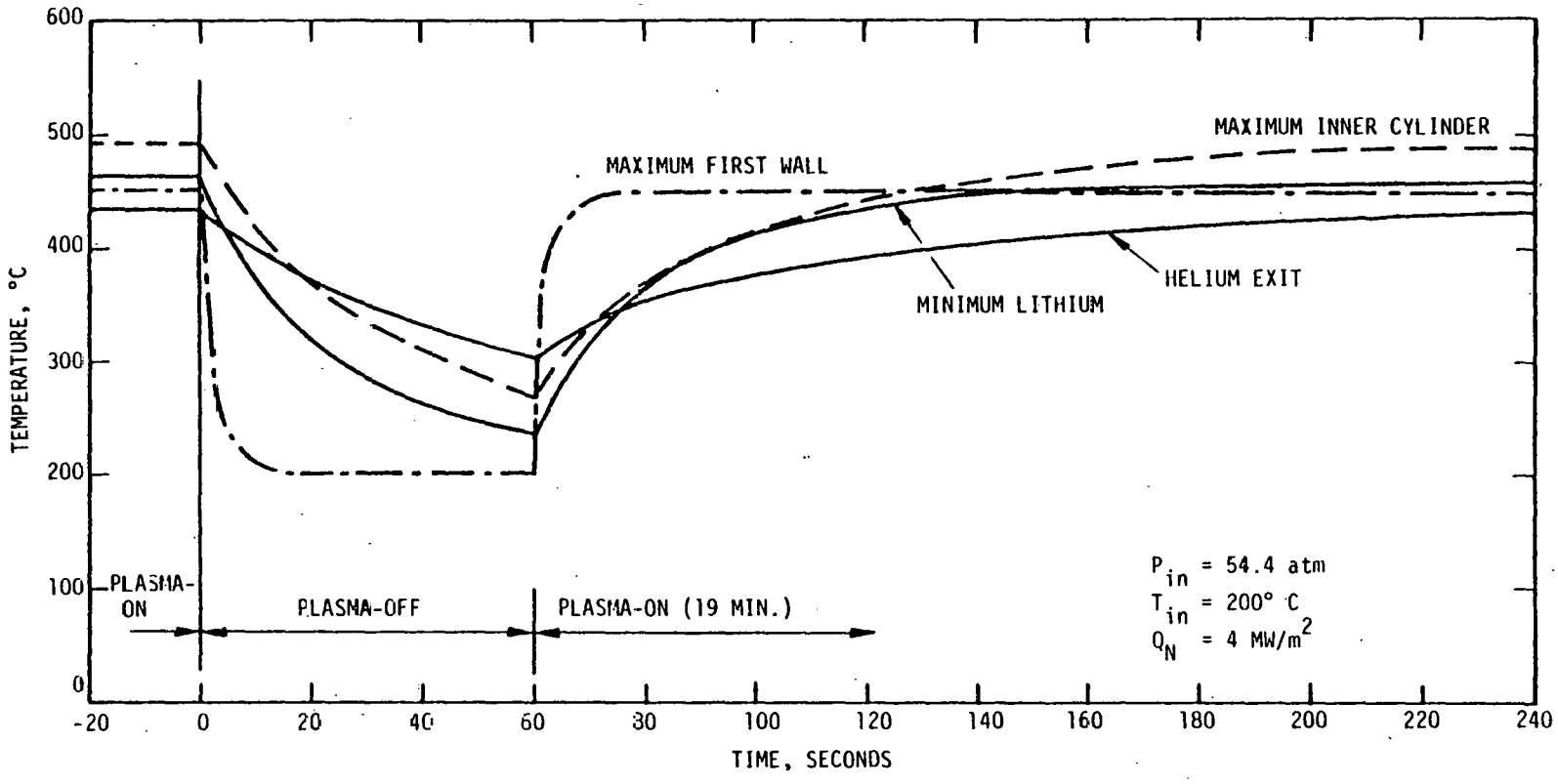

Figure 5.4-1. Transient Thermal Conditions During a Plasma-Off and On Cycle.

5.5 PERFORMANCE WITH A DIVERTOR

If the reactor utilizes a divertor for impurity control, the particle heat flux on the first wall will in the limit be zero. The module thermal loading then consists only of the nuclear heating due the 4 MW/m^2 neutron wall loading. The performance curves of the module without the particle heat flux with the helium inlet temperature of 200° C and 250° C are shown in Figure 5.5-1. In this figure the maximum inner cylinder temperature and the maximum first wall temperature were plotted against the pumping power and the helium exit temperature was plotted against the maximum inner cylinder temperature only. Since the first wall is not heated by the particle flux, the limiting structural temperature occurs at the inner cylinder. When the inner cylinder is operated at a maximum value of 500° C with the helium inlet temperature at 200° C, the maximum first wall temperature is 270° C, the helium exit temperature is 440° C and the required pumping power is about 1.25% as shown by the circles connected by the dotted line. If the helium inlet temperature is increased to 250° C, the maximum first wall temperature would be slightly higher, but the required pumping power is more than doubled.

Comparing the performance with and without a divertor, the effect is a much lower first wall temperature and lower pumping power requirement with a divertor. The helium exit temperature remains the same, and is limited by the allowable inner cylinder structure temperature.

5.6 PERFORMANCE OF A 19 cm DIAMETER MODULE

From the results shown in Table 5.1-1 it is seen that the maximum steady state lithium temperature is well below its boiling point in a 10 cm O. D. module. Since it is desirable to increase the module size to reduce the total number of modules required in a reactor, the feasibility of designing a larger module was investigated. The results are given below.

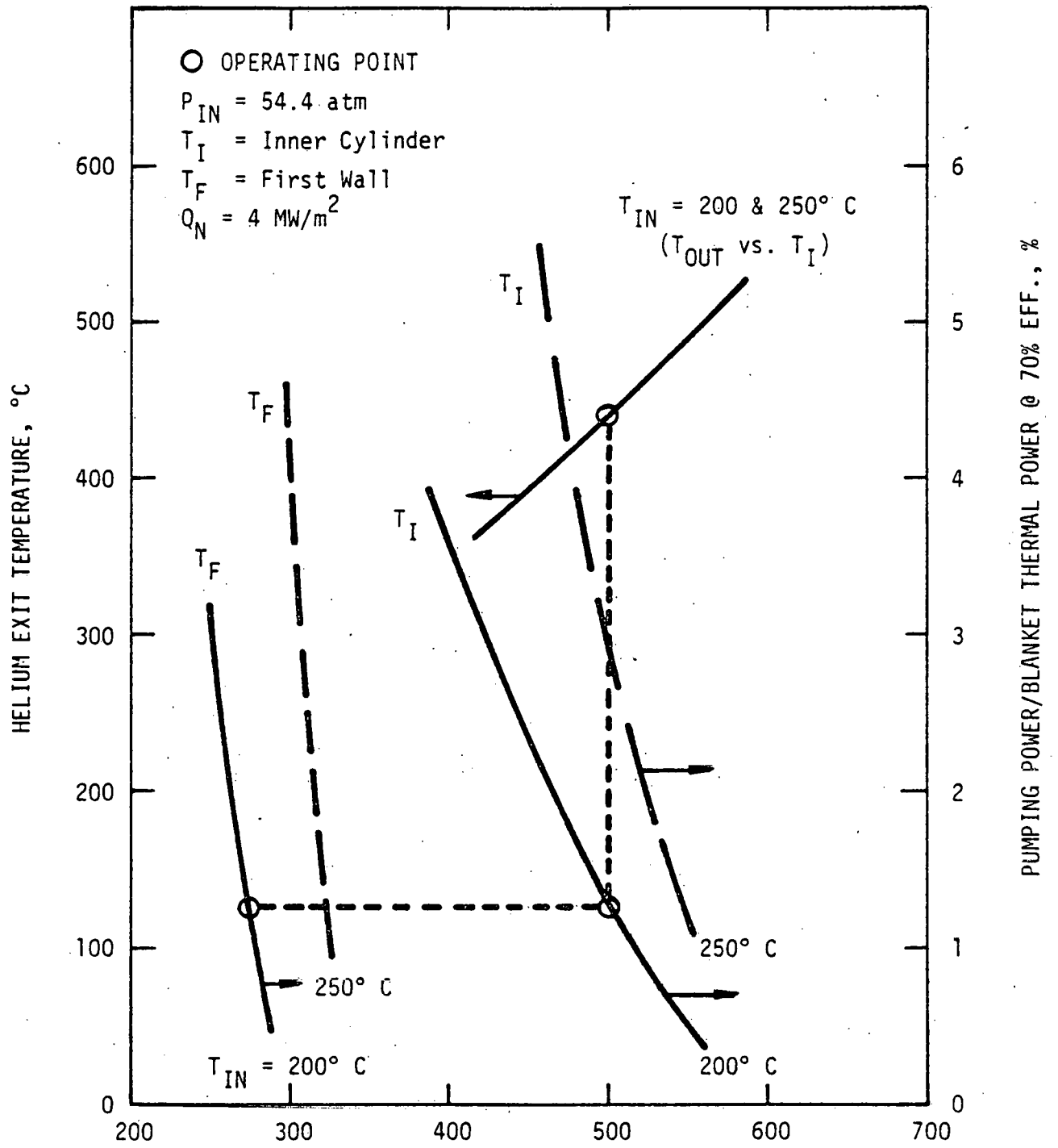

Figure 5.5-1. Steady State Performance Curves of Module with Divertor in Reactor

Consider a long and uniform solid cylinder of radius r_o with a constant internal heat generation rate Q''', the maximum center line temperature is calculated from the following equation:

$$T_{max} = T_f + \frac{Q'''}{2k}\left(\frac{r_o^2}{2} + \frac{kr_o}{h}\right) \tag{9}$$

Utilizing the same hydraulic conditions of the reference case at the location where the inner cylinder temperature is maximum: T_f = 325° C, k = .377 W/cm-C, for lithium h = 0.172 W/cm^2-C and Q''' = 11.5 W/cm^3, if T_{max} is limited to 1300° C which is slightly below the boiling temperature of the lithium, from Equation (9), r_o was caluclated to be about 9.3 cm, or the module diameter is about 18.6 cm. This indicates that a cylinder with almost twice the diameter of the current module can have the maximum lithium temperature at the center line still below the boiling point. However, using the same helium coolant temperature and heat transfer coefficient given above, the wall temperature of the larger cylinder calculated by the following equation:

$$T_w = T_f + \frac{Q'''r_o}{2h} \tag{10}$$

comes out to be 675° C which is higher than the allowable limit of 500° C. In order to lower the wall temperature to 500° C, the heat transfer coefficient must be doubled by increasing the coolant flow rate. This means that the pumping requirement will be much higher than the 2.2 % required for the 10 cm O.D. module.

From the above simplified analysis it can be concluded that since the maximum inner cylinder wall temperature of the present design is already close to the limit of 500° C, the module cannot be made much larger than 10 cm without increasing the pumping power requirement. Optimization of the flow gap sizes could still be considered to increase the heat transfer coefficient without increasing the flow rate significantly. Since the pumping power is proportional to the third power of the flow rate, a slight increase in flow rate results in considerable increase in the pumping power requirement. It appears that the 10 cm diameter cannot be increased significantly for a module under the given design guidelines and requirements.

6.0 OFF-DESIGN POINT PERFORMANCE

The thermal performance of the module at the following three off-design conditions were analyzed: (1) coolant flow variation and loss of coolant, (2) part load operation, and (3) hypothetical plasma disruption. At each of these off-design conditions only a few selected cases were investigated because of the limited scope of this study. The nominal operating conditions of the module were discussed in Section 5.2. The results of the off-design performance analysis are presented in the following subsections.

6.1 COOLANT FLOW VARIATION AND LOSS OF COOLANT

Since there are a great number of modules in the blanket region with many parallel flow paths, the possibility that some coolant flow deviation from the nominal would occur in some modules was considered. The steady state thermal conditions of the module with coolant flow variation from 30% to 140% of the nominal flow rate are shown in Figure 6.1-1. If the absolute maximum of the structure temperature under steady state is 550° C as stated in the design guidelines, the module can be operated with up to -20% of the nominal flow. At this reduced flow rate, the maximum inner cylinder temperature just reaches the limit, but the maximum first wall temperature is about 500° C. Since the maximum first wall temperature limit is $\sim$ 450° C, the module may tolerate a coolant flow reduction of about -10% as the limit. The maximum lithium temperature would not reach the boiling point, until the coolant flow is reduced to less than 30% of the nominal value.

In a loss of coolant fault condition, it was assumed that the coolant is reduced to 1% of the nominal value in one second. The maximum first wall and the maximum inner wall temperature during this transient are shown in Figure 6.1-2. The first wall reaches 700° C in about one second if the plasma continues to be on. If the plasma termination could be completed in less than one second after the loss of coolant is detected, the first wall temperature would not reach the 700° C level but starts to drop as soon as the

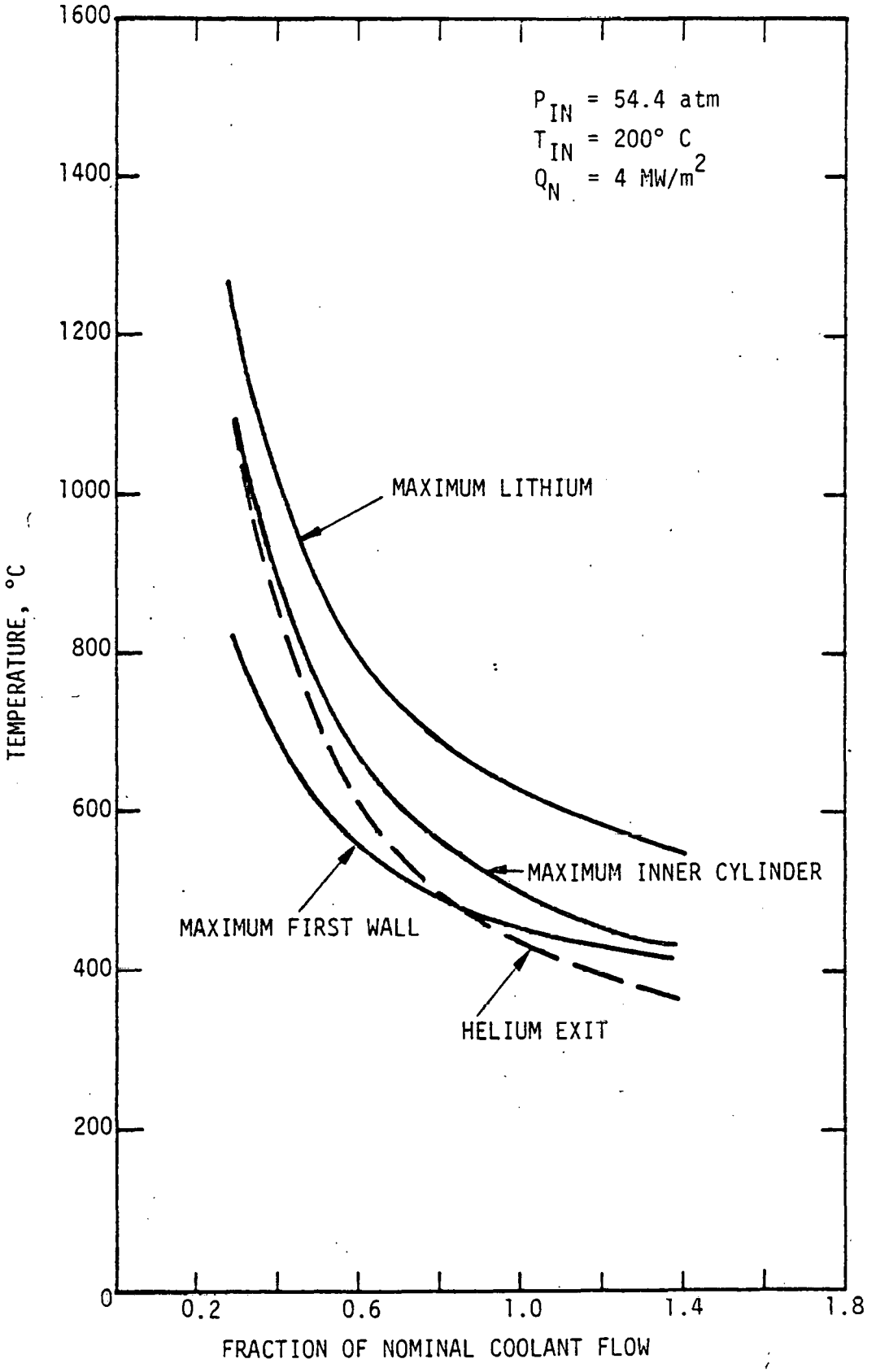

Figure 6.1-1. Effect of Variation in Coolant Flow on Module Steady State Temperatures.

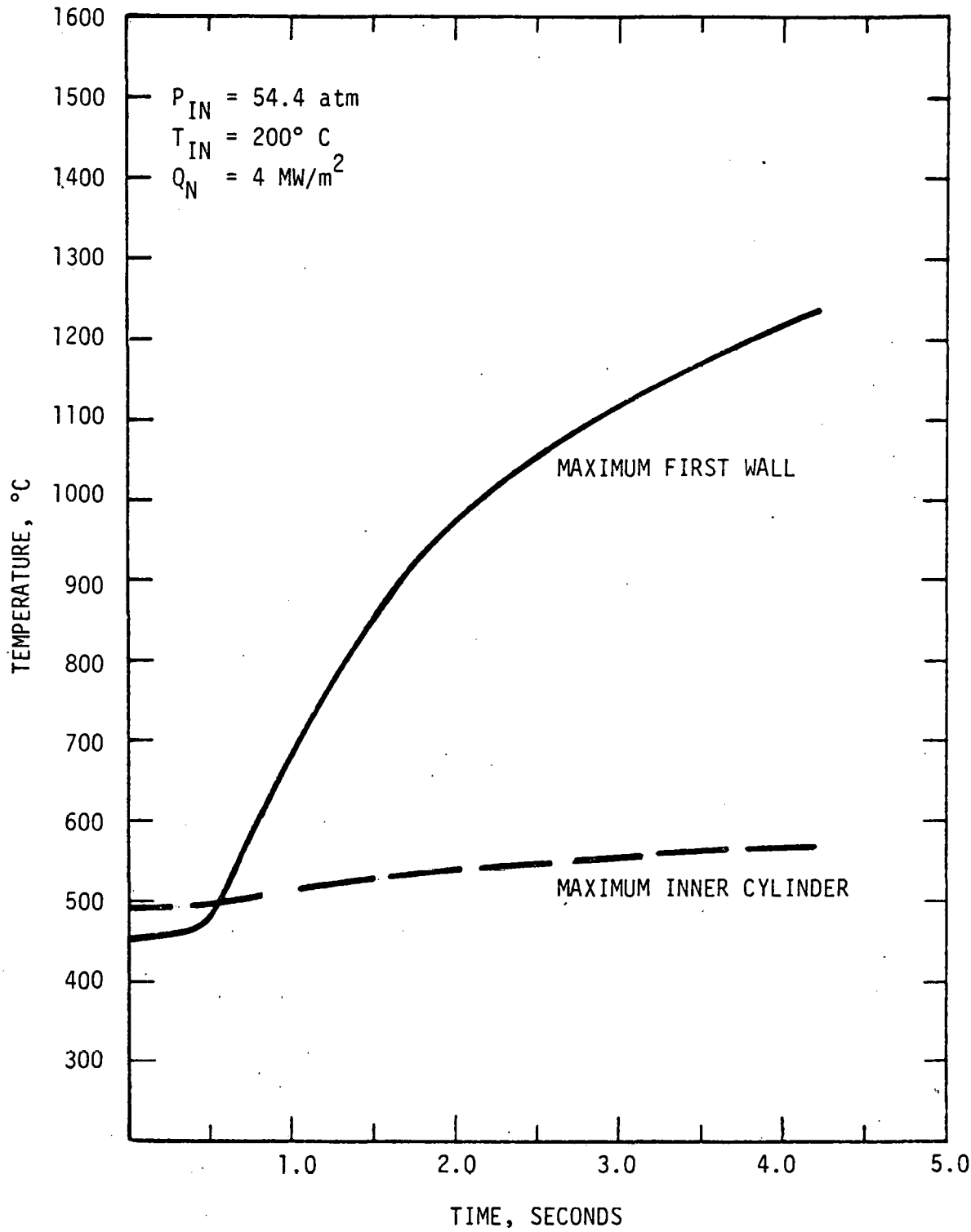

Figure 6.1-2. Structural Temperature Response to Loss of Coolant to 1% of Nominal Flow in One Second.

plasma is terminated. The inner cylinder temperature response is very slow, therefore the ability of the inner cylinder to contain the liquid lithium should be maintained. Since it may not be feasible to monitor every module in the blanket region, means for detecting such fault condition would have to be developed.

6.2 PARTIAL POWER CONDITIONS

At partial power operations if the coolant flow rate were to remain the same as in full power condition, the helium exit temperature would decrease and the module would be overcooled. In order to operate the module to its full thermal potential at partial power, the coolant flow rate should be reduced accordingly. The thermal conditions of the module at 50% neutron wall loading (2 MW/m^2) with two different helium inlet pressures and temperatures were analyzed. The performance curves are plotted as shown in Figures 6.2-1 and 6.2-2. The curves were plotted in the same manner as those discussed in Section 5 (for example, Figure 5.5-1). Figure 6.2-1 shows the operating lines at T_{IN} = 200° C. Because of the reduced wall loading the module can be operated with lower coolant flow and at a lower pressure. To operate at a helium pressure of 35 atm with the maximum inner cylinder temperature of 500° C, the required pumping power is about 1.1%. The corresponding maximum first wall temperature is 420° C and the helium exit temperature is 450° C as shown by the circles in the figure. If the helium pressure is increased to 54.4 atm, the required pumping power is further reduced to about 0.5%.

The operating lines for the cases with helium inlet temperature at 250° C are shown in Figure 6.2-2. To operate at a helium inlet pressure of 35 atm and the maximum inner cylinder temperature of 500° C, the required pumping power becomes about 2.1%. The corresponding maximum first wall is 440° C and the helium exit temperature is 465° C. The higher coolant temperatures would provide a better power conversion efficiency. The thermal performance gains of this module design to operate with a reduced wall loading are in the direction of reduced pumping power requirement and higher coolant temperatures.

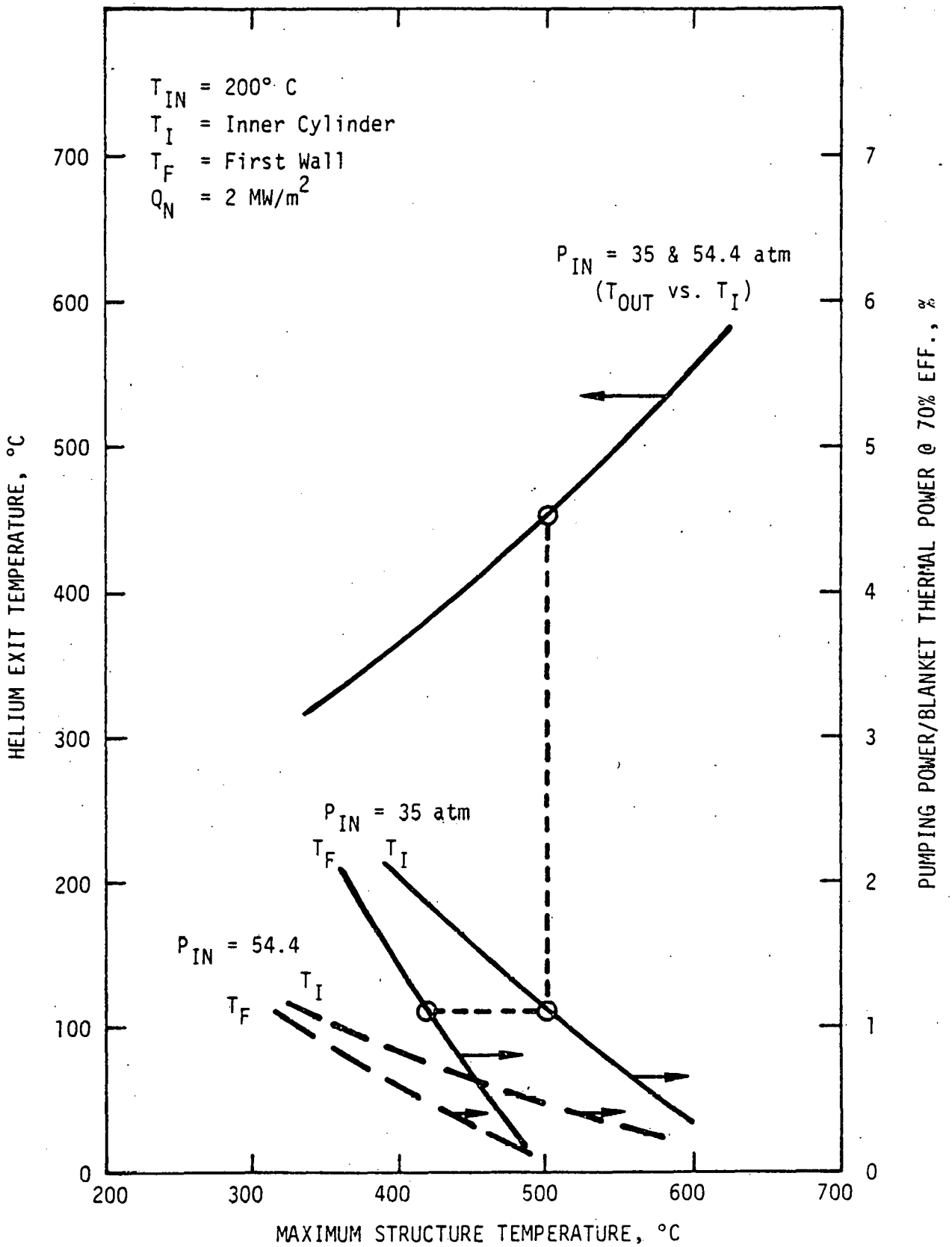

Figure 6.2-1. Steady State Performance Curves of Module at Partial Power Condition with T_{IN} = 200° C

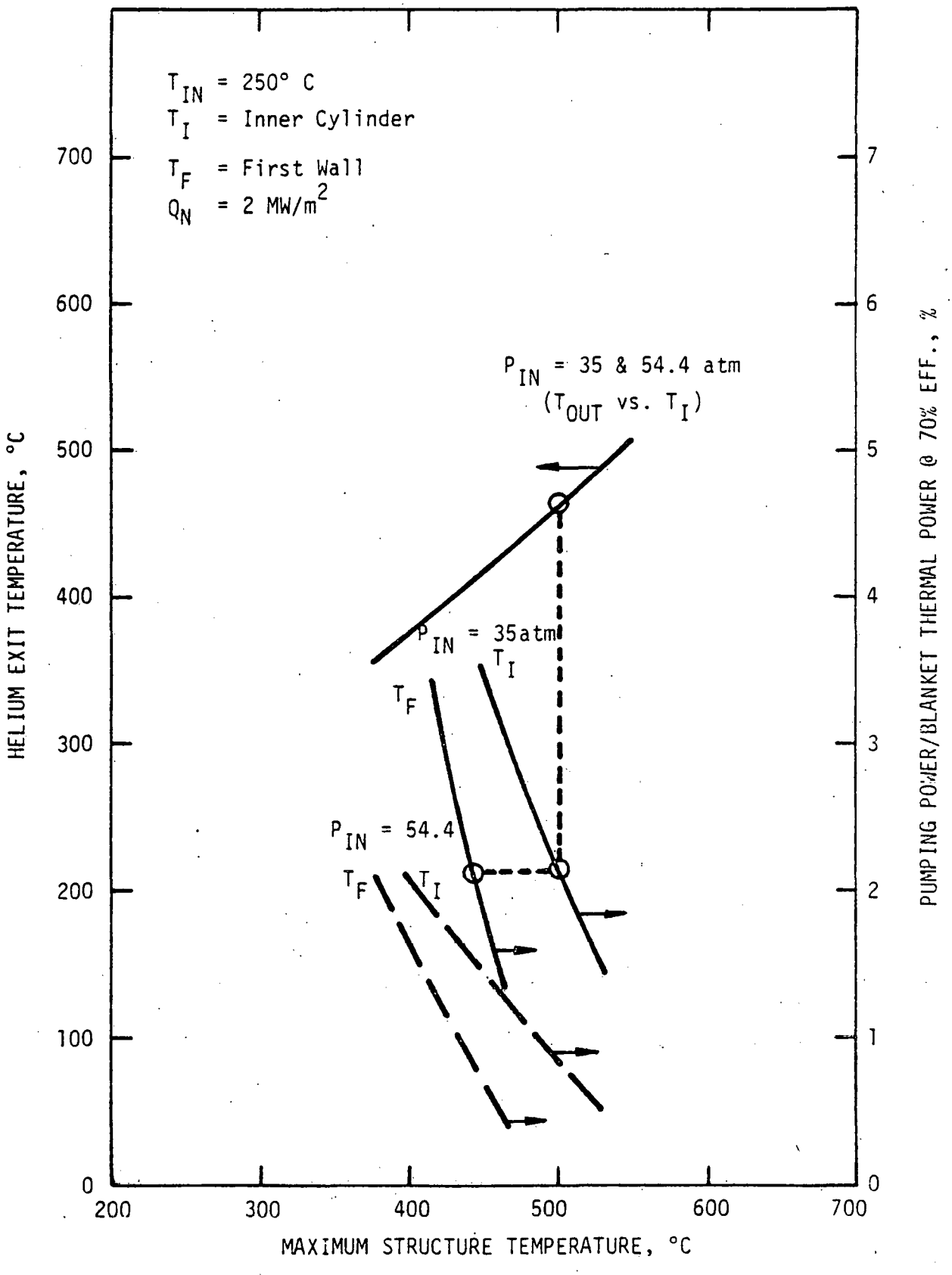

Figure 6.2-2. Steady State Performance Curves of Module at Partial Power Condition with T_{IN} = 250° C

6.3 SIMULATED PLASMA DISRUPTION

Since the scenario for a plasma disruption condition is not well defined for this analysis, the first wall temperature responses to various levels of particle heat flux up to 80 MW/m^2 for 0.010 second were calculated. The temperatures at the end of the 0.010 second transient are shown in Figure 6.3-1. It is seen from the figure that the surface temperature increases rapidly with heat flux, but the bulk average temperature of the cylinder increase is small for a heat pulse of this duration. The surface temperature would reach the melting point with a heat flux in the order of 80 MW/m^2. The resulting thermal stresses from the high temperature difference between the surface and the bulk of the material would have to be evaluated to determine whether allowable stresses would be exceeded prior to reaching melting temperatures at the first wall surface.

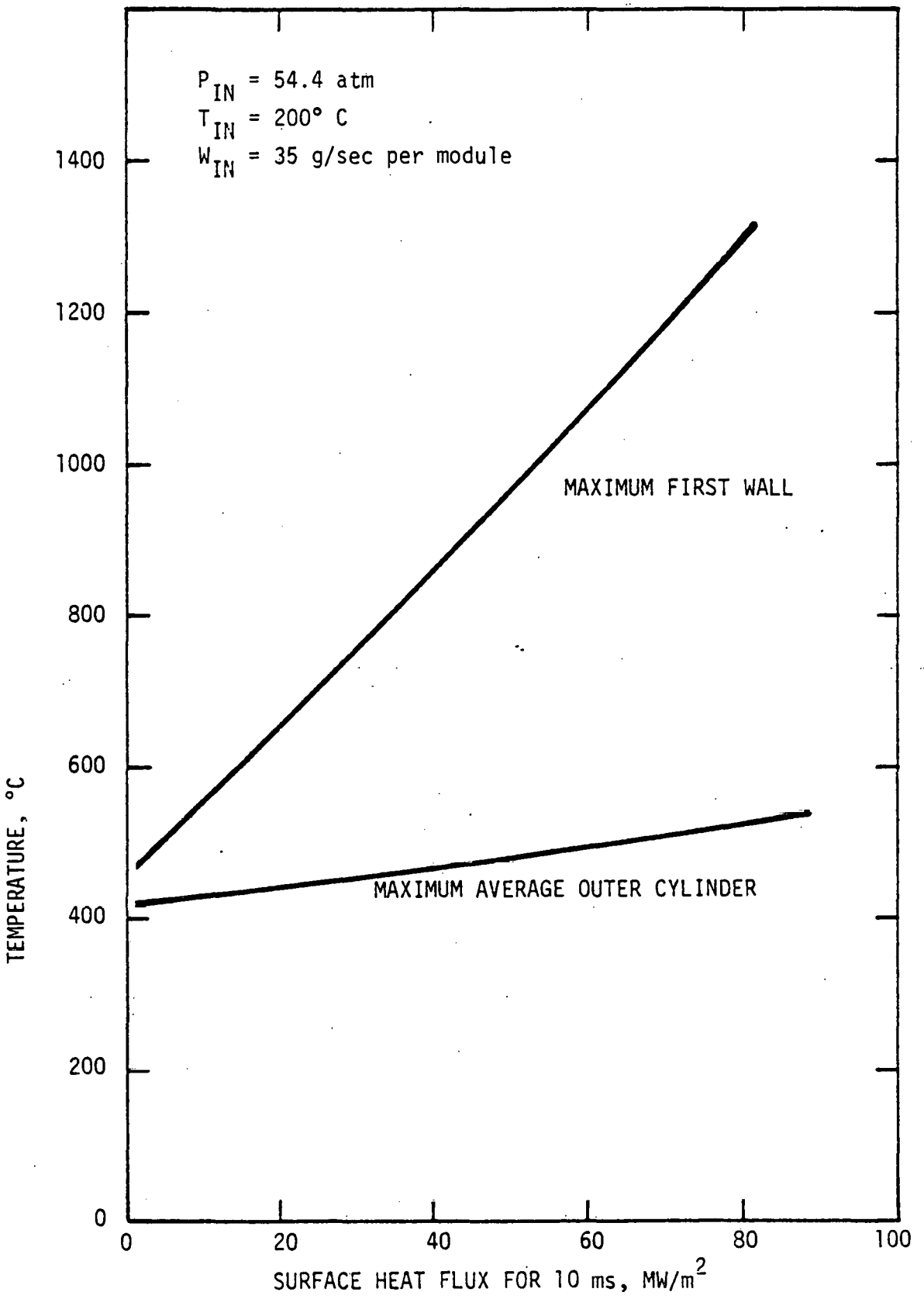

Figure 6.3-1. First Wall Temperature Response to Heat Flux.

7.0 NOTATIONS

A = channel flow area, cm^2

C_p = Specific heat at constant pressure, J/g-C

D = Hydraulic diameter, cm

f = Fanning friction factor

G = mass velocity, $g/sec\text{-}cm^2$

g = Gravitational constant, cm/sec^2

H = Enthalpy, J/g

h = Heat transfer coefficient, $W/cm^2\text{-}C$

J = Mechanical equivalent of heat, 4.185 J/g-cal.

k = Thermal conductivity, W/cm-C

p = Pressure, kgf/cm^2

P = Wetted perimeter, cm

Q = Heat flux, W/cm^2

Q''' = Nuclear heat generation rate, W/cm^3

ρ = Density, g/cm^3

T = Temperature, C (T_f = Coolant Temperature, T_W = Wall Temperature)

v = specific volume, cm^3/g

Nu = Nusselt number

Re = Reynold number

Pr = Prandtl number

x, y, z = cartesian coordinates

8.0 REFERENCES

1. J. S. Karbowski, et al., "Tokamak Blanket Design Study: FY 78 Summary Report," ORNL/TM-6847 (to be published).

2. T. V. Prevenslik, "Structural Evaluation of a Tokamak Reactor Cylindrical Module Blanket Concept," WFPS-TME-096, October, 1978 (to be published).

3. G. W. Ruck, "Design Development of a Tokamak Reactor Cylindrical Module Blanket Concept," WFPS-TME-105, October, 1978 (to be published).

4. B. L. Pierce and C. A. Holden, "The Thermodynamic and Transport Properties of Helium for Use in Evaluation of Closed Cycle Brayton Systems," WANL-TME-2879, October, 1976.

5. W. H. McAdams, "Heat Transmission," Third Edition, McGraw Hill, New York, p. 219, 1954.

6. W. H. McAdams, "Heat Transmission," Third Edition, McGraw Hill, New York, p. 155, 1954.

7. W. M. Rohsenow, editor, "Handbook of Heat Transfer," Sections 7 and 10, McGraw-Hill, New York, 1973.